Spherical microparticles with Saturn ring defects and their self-assembly across the nematic to smectic-*A* phase transition

K. P. Zuhail,[1] S. Čopar,[2] I. Muševič,[2,3] and Surajit Dhara[1,*]

[1]*School of Physics, University of Hyderabad, Hyderabad-500046, India*

[2]*Faculty of Mathematics and Physics, University of Ljubljana, Jadranska 19, SI-1000 Ljubljana, Slovenia*

[3]*Condensed Matter Physics Department, Jožef Stefan Institute, Jamova 39, 1000 Ljubljana, Slovenia*

(Received 4 August 2015; published 2 November 2015)

We report experimental studies on the Saturn ring defect associated with a spherical microparticle across the nematic (N) to smectic-A (SmA) phase transition. We observe that the director distortion around the microparticle changes rapidly with temperature. The equilibrium interparticle separation and the angle between two quadrupolar particles in the N phase are larger than those of the SmA phase. They are almost independent of the temperature in both phases, except for a discontinuous jump at the transition. We assembled a few particles using a laser tweezer to form a two-dimensional colloidal crystal in the N phase. The lattice structure of the crystal dissolves irreversibly across the N-SmA phase transition. The results on the pretransitional behavior of the defect are supported by the Landau–de Gennes Q-tensor modeling.

DOI: 10.1103/PhysRevE.92.052501 PACS number(s): 61.30.Jf, 64.70.M−

I. INTRODUCTION

Dispersion of particles with predefined surface anchoring in an aligned nematic liquid crystal (NLC) creates elastic distortion of the director around the particle [1–6]. The distortions culminate in the appearance of a topological defect in the neighborhood of each particle and mediate long-range forces, which opens up new directions in colloidal assembly [7–12]. These have been the subject of intensive research during recent years [13–21]. Such colloidal assemblies are significantly different from the spatial aggregation of colloidal particles in isotropic fluids, which are mostly governed by the electrostatic, sterical, and van der Waals interactions. The forces in liquid crystals are of elastic origin and extend over several micrometers [1–4].

When the microparticles are treated to promote the perpendicular alignment of liquid crystal molecules, two different defect configurations can be stabilized. In analogy with the electric field, depending on the far-field symmetry, these "elastically charged" objects are called elastic dipoles and quadrupoles [2–4]. In the elastic dipole a hyperbolic hedgehog defect of strength -1 is associated with each microparticle, whereas in the case of the quadrupole, a Saturn ring defect of strength $-1/2$ encircles the microparticle. The interaction potential between a pair of dipoles and quadrupoles varies as r^{-3} and r^{-5}, respectively [10].

Most of the experimental investigations are carried out in nematic or cholesteric liquid crystals. We recently studied colloidal particles with hyperbolic hedgehog and boojum defects across the N-SmA phase transition. We showed that both types of nematic defects are transformed into focal conic line defects in the SmA phase [22,23]. The phase transition has a strong influence on the pairwise colloidal interaction and is responsible for structural transitions in two-dimensional colloidal crystals. In this paper, we report on studies of colloidal particles with Saturn ring defects across the N-SmA phase transition. We investigate the effect of elasticity on the pretransitional structure of a pair of quadrupolar colloids with Landau–de Gennes Q-tensor modeling. We find that the temperature dependence of interparticle separation and the angle of their joining line with respect to the rubbing direction are insensitive to the elastic anisotropy. This is in sharp contrast with our previous observations on the dipole and boojum defects.

II. EXPERIMENTAL

We used Silica microspheres of diameter 5.2 and 8 μm (Bangs Laboratory, USA) coated with octadecyldimethyl-3-trimethoxysilylpropyl-ammonium chloride (DMOAP) to induce strong homeotropic anchoring of liquid crystal (LC) molecules. The particles were dispersed in 8CB liquid crystal (4'-*n*-octyl-4-cyano-biphenyl) which exhibits the following phase transitions: Cr (crystal) 21.5 °C SmA (smectic-A) 33.5 °C N (nematic) 40.5°C I (isotropic). The colloidal mixture is introduced into a glass cell coated with polyimide Al-1254 and rubbed in an antiparallel way to induce planar alignment of LC molecules. A laser tweezer was built around an inverted optical polarizing microscope (Nikon Eclipse Ti-U) using a cw solid-state laser operating at 1064 nm (Aresis, Tweez 250Si). An acousto-optic deflector interfaced with a computer was used for trap movement. The temperature of the sample was controlled by a heater and a proportional-integral-derivative (PID) controller with an accuracy of ±0.1 °C. A camera (CCD, iDs-UI) with a frame rate of 20 frames per second was attached to the microscope for video recording. A particle tracking program was used to measure the particles' coordinates in time with a resolution of ±10 nm.

III. RESULTS AND DISCUSSION

Figure 1 shows the transformation of a Saturn ring defect across the N-SmA phase transition. There are four visible colored lobes of distortion around the particle in the N phase, and these lobes elongate as the N-SmA transition point is approached [Figs. 1(a) and 1(b)]. Just below the transition, the lobes shrink to narrow stripes emanating from

*Email: sdsp@uohyd.ernet.in

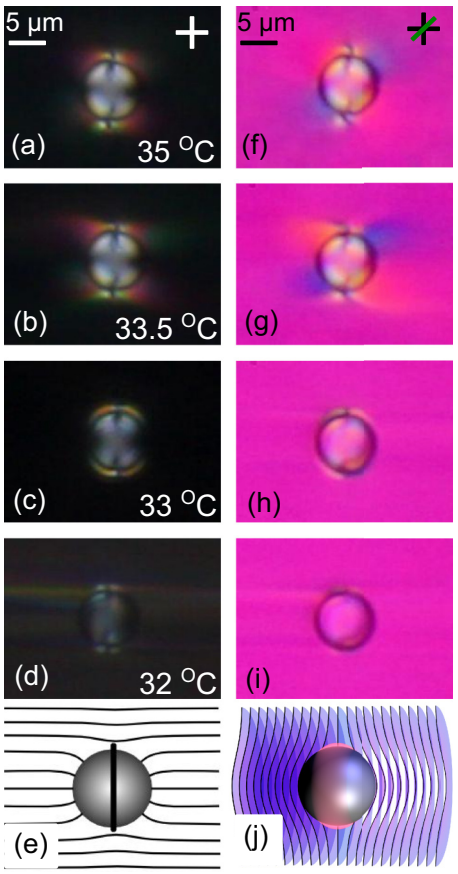

FIG. 1. (Color online) (a)–(d) Optical photomicrographs (obtained from polarizing optical microscopy) of a quadrupolar colloidal particle of diameter 8 μm in an 8CB filled cell of thickness 11 μm under crossed polarizers at various temperatures across the N-SmA phase transition. See Supplemental Material, video 1 (f)–(i) [26]. Corresponding images with the red wave-plate (green line denotes the slow axis) between the analyzer and the sample. Note that the blue and yellow colors have exchanged their positions around the microsphere in the SmA phase [in Fig. 1(h)] due to higher-order effects. (e) The streamlines of the director above the transition. (j) In the smectic phase, the boundary condition is incompatible with the layer structure at the equator, where the Saturn ring was present in the nematic phase. Note that the layer thickness is greatly exaggerated.

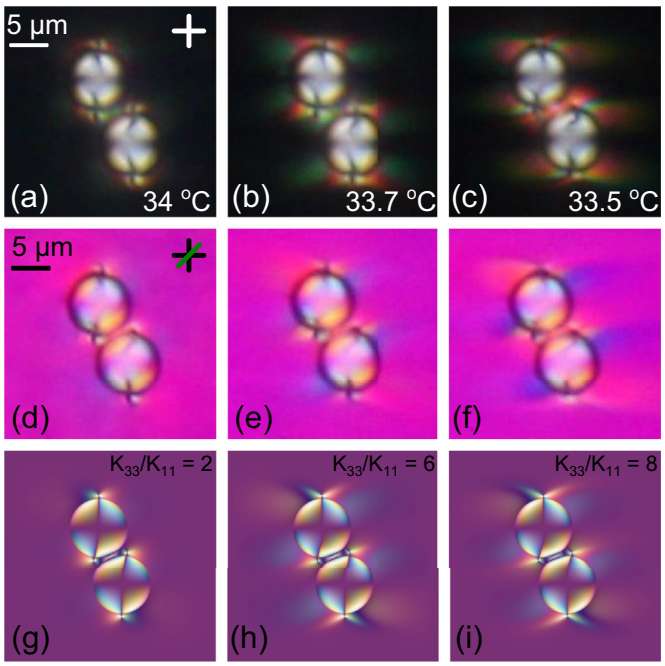

FIG. 2. (Color online) (a)–(c) Optical photomicrographs just before the N-SmA phase transition of 8-μm homeotropic microsphere in a planar cell. Cell thickness: 11 μm. (d)–(f) Photomicrographs with red wave-plate between the sample and the analyzer in the N phase. (See Supplemental Material, video 2 [26].) (g)–(f) Simulated images with the wave plate at various ratios of K_{33}/K_{11}.

a barely visible ringlike remnant of the nematic defect on the surface of the microparticle [Fig. 1(c)]. Further down from the transition temperature the ring almost disappears [Fig. 1(d)]. A few images were taken between crossed polarizers, with an additional λ plate (red wave-plate) inserted between the sample and the polarizer to reconstruct the molecular orientation around the microsphere. The red color corresponds to a horizontal orientation of the long molecular axes, whereas bluish and yellowish colors correspond to anticlockwise and clockwise rotation of the director from the rubbing direction, respectively. By analyzing these images we can conclude that the director distortion around the microparticle expands before the N-SmA phase transition, and then in the SmA phase the distortion is highly confined into a narrow region at the equator of the particle, as layer stiffness prevents an extensive deformation [Fig. 1(c)]. Video I in our Supplemental Material clearly shows this transformation [26]. As the temperature is reduced further into the SmA phase, the ring fades away and two horizontal faint bands appear below and above the microparticle (see video I [26]). These bands are the distorted regions in which the SmA layer normal is slightly tilted with respect to the rubbing direction. This appears due to the imposition of strong homeotropic anchoring of the SmA layers on the surface of the microsphere. Careful observation suggests that the SmA layers in the bands have opposite tilt. A schematic representation of the director in the N phase corresponding to the Saturn ring shown in Fig. 1(a) and the confined Saturn ring in the SmA phase corresponding to the state shown in Fig. 1(c) are shown in Figs. 1(e) and 1(j), respectively. The shaded equatorial band in Fig. 1(j) roughly marks the thin near-surface region where the boundary condition violation is reconciled in a way that cannot be directly deduced from the micrographs.

In the nematic phase, a pair of colloidal particles with quadrupole defects are manipulated using laser tweezers and observed across the N-SmA phase transition. A few representative images are shown in Fig. 2. The size of the lobes representing the director distortion increases as the N-SmA transition point is approached. Since the splay elastic constant (K_{11}) remains constant, the pretransitional structure of the quadrupole is due to the increase in the bend elastic constant near the N-SmA phase transition. To confirm that the increase in the elastic constant ratio is the main reason, we performed numerical simulation using Landau–de Gennes Q-tensor modeling in the N phase, as in Ref. [22]. The free

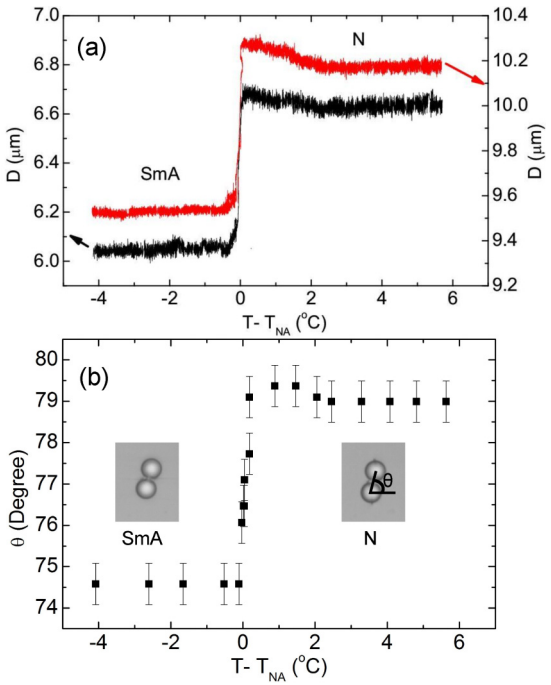

FIG. 3. (Color online) (a) Variation of center-to-center separation (D) between a pair of colloidal particles across the N-SmA phase transition. The red and black color corresponds to particle diameters of 8 and 5.2 μm, respectively. (b) Variation of θ with temperature across the N-SmA phase transition.

energy density in the form

$$f = \frac{A}{2}Q_{ij}Q_{ji} + \frac{B}{3}Q_{ij}Q_{jk}Q_{ki} + \frac{C}{4}(Q_{ij}Q_{ji})^2 + \frac{L_1}{2}(Q_{ij,k})^2 + \frac{L_3}{2}Q_{ij}Q_{kl,i}Q_{kl,j} \quad (1)$$

was minimized on a finite difference grid. The phase parameters were set at $A = -0.172 \times 10^6$ N m^{-2}, $B = -2.12 \times 10^6$ N m^{-2}, $C = 1.73 \times 10^6$ N m^{-2}. The tensorial elastic constants L_i relate to the Frank constants via the relations $L_1 = \frac{2}{27S^2}(2K_1 + K_3)$, $L_3 = \frac{4}{27S^3}(-K_1 + K_3)$, assuming $K_2 = K_1$ and S being the equilibrium bulk order parameter [24,25]. We set $L_1 = 4 \times 10^{-11}$ N and varied the ratio K_{33}/K_{11}. The simulated cell was 1.4-μm thick and the particle diameter was 0.9 μm. The corresponding images with increasing ratio of K_{33}/K_{11} are shown in Fig. 2, where the effect is qualitatively reproduced.

We also measured the equilibrium interparticle separation (D) across the N-SmA phase transition. The temperature variation of D is shown in Fig. 3. We observe that above $T - T_{NA} = 3\,^\circ$C, D is independent of temperature and it increases slightly below this temperature. At the N-SmA phase transition D changes discontinuously, marking the discontinuity of the elastic constants of the N phase. For example, in the N phase (5.2-μm particles), 4 °C above the N-SmA transition point, $D \simeq 6.8$ μm and in the SmA phase, $D \simeq 6.2$ μm. This can be contrasted with the past experiments with different defect states accompanying the particles: for dipolar colloids [22], it was found that the interparticle separation increases linearly with the elastic anisotropy. In

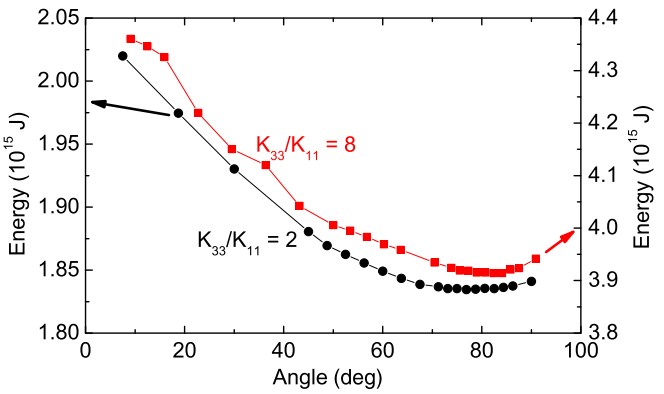

FIG. 4. (Color online) Variation of the free energy with the angle (θ) at two different ratios of K_{33}/K_{11} obtained by Landau–de Gennes modeling for the nematic phase. The free energy minimum is around 79° for both ratios.

the case of boojums [23], D decreases linearly with the elastic anisotropy. Thus the separation between a pair of microspheres is governed by the type of the associated defect and the elastic anisotropy.

We also measured the angle between the rubbing direction and the joining line of the centers of the two particles with temperature [Fig. 3(b)]. The angle (θ) is larger in the N phase compared to the SmA phase and discontinuously changes across the phase transition. For example, in the nematic and SmA phases, the angles are $\theta \simeq 79 \pm 1^\circ$ and $74.5 \pm 1^\circ$, respectively. We calculated the free energy profiles for two different ratios of K_{33}/K_{11} in the N phase using Landau–de Gennes theory (Fig. 4). It is observed that the equilibrium angle in both cases is about $\simeq 79 \pm 3^\circ$, which is comparable to the experimental values.

When a pair of colloidal particles are assembled and cooled into the SmA phase, two long and dark tails, asymptotically parallel to the rubbing direction, appear [Fig. 5(a)]. The brighter regions on both sides of the tails indicate that the layers are strongly bent. The tails are focal conic line defects similar to those reported recently [22,23], which is supported by the molecular orientation inferred from the photomicrograph with an inserted red-plate between the sample and the polarizer [Fig. 5(b)]. A schematic representation of the SmA layer structure around the colloids is shown in Fig. 5(c).

Finally, we show the effect of the N-SmA phase transition on a two-dimensional quadrupolar colloidal crystal. We

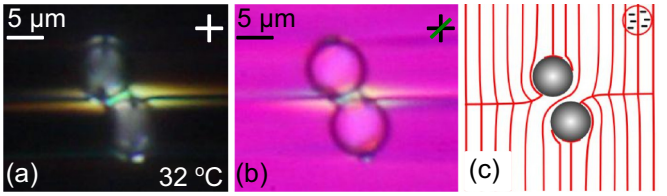

FIG. 5. (Color online) Optical photomicrographs of a pair of colloidal particles in the SmA phase (at T-$T_{NA} = -1\,^\circ$C), without (a) and with (b) the wave plate. The blue and yellow colors around the microsphere in the SmA phase are second-order colors. Particle diameter: 8 μm. (c) A sketch of the smectic layer arrangement with marked focal lines that are visible in the photomicrographs.

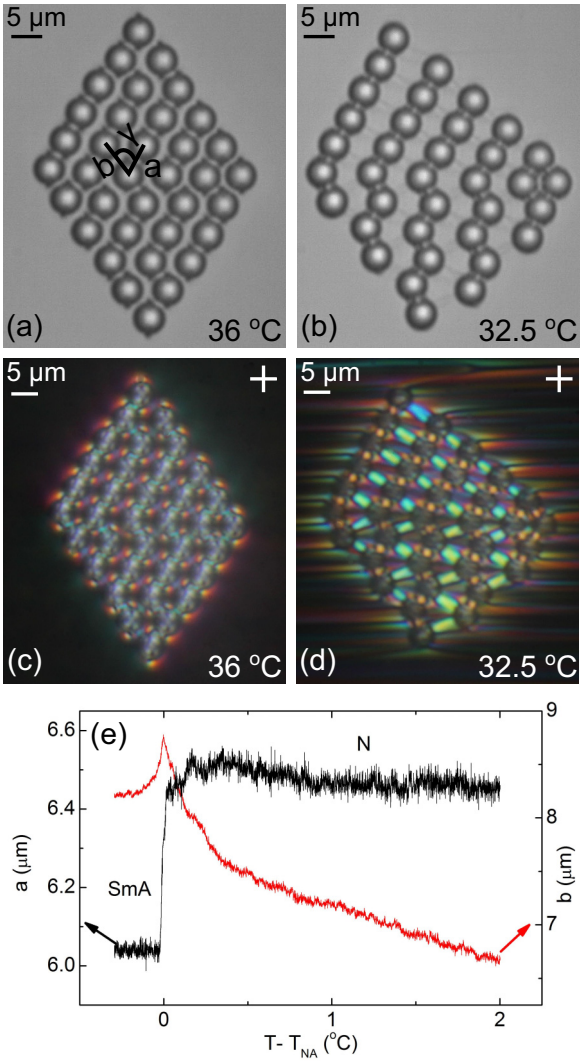

FIG. 6. (Color online) Optical photomicrographs of a 2D quadrupolar crystal in the (a, c) N phase (36 °C) and (b, d) SmA phase (32.5 °C) of 8CB liquid crystal; (a,b) without polarizers and (c, d) with crossed polarizers. Particle diameter 5.2 μm, and cell thickness 8 μm. (e) Temperature variation of lattice parameters a and b across the N-SmA transition (see Supplemental Material, video 3 [26]).

assembled 36 quadrupolar particles with the help of a laser tweezer and prepared a two-dimensional (2D) quadrupolar crystal following the procedure reported in Ref. [2]. The sample was cooled across the N-SmA phase transition at a rate 0.3 °C/min (see Supplemental Material, video 3). Figure 6 shows the optical micrographs of the 2D crystal in the N and SmA phases. In N phase [Fig. 6(a)] the crystal exhibits an oblique unit cell with lattice parameters $a = 6 \pm 0.05$ μm, $b = 6.3 \pm 0.05$ μm, and $\gamma = 64^\circ \pm 1^\circ$, and this is consistent with the previous report [2]. When the temperature is reduced, the crystal expands laterally and then in the SmA phase completely breaks apart into chains of various lengths perpendicular to the rubbing direction. There are some kind of bondlike links observed between the neighboring microspheres in the SmA phase. Careful observation suggests that in the bond region the SmA layers are parallel between the two surfaces of the microparticles. Using a particle tracking program, we measured the lattice parameters, shown as a, b in Fig. 6(c). The lattice parameter a remains nearly constant, while b increases rapidly and reaches to a maximum value before decreasing in the SmA phase. In the N phase there is a strong bend deformation between the neighboring chains [2]. The divergence of b is expected due to the expulsion of the bend distortion as the SmA phase is approached. This is somewhat similar to what was observed in case of dipolar colloidal crystal [22,23]. However, there are certain different features of this structural transition compared to that observed in the case of dipole and boojum colloidal crystals. The main difference is that in the previous systems we observed a reversible structural transition in both heating and cooling. The structure changed from oblique in the N phase to a hexagonal lattice in the SmA phase. In the case of quadrupolar crystal, it is irreversible, i.e., the crystal lattice is broken in the SmA phase while cooling and it does not rearrange while heated back to the N phase. This could be due to the much lower binding energy (∼10 times) of the quadrupolar crystals compared to dipolar crystals.

IV. CONCLUSIONS

In conclusion, we studied the transformation of a Saturn ring defect across the N-SmA phase transition. The director distortion around the particle changes continuously due to the pretransitional increase in the ratio of the bend and splay elastic constants. The Saturn ring in the SmA phase transforms into a barely visible localized near-surface defect region. The sharp discontinuity of the nematic elastic constants across the phase transition is reflected in the equilibrium separation and angle between the two particles. For a pair of particles the experimental observations are supported by numerical simulations in the nematic phase. In the SmA phase long focal conic line-defects are observed on both sides of the dimer. The long-range distortion in the direction of the focal lines interferes with the integrity of the oblique lattice of 2D quadrupolar particles, which breaks irreversibly at the transition into the smectic phase. The irreversible structural transition indicates that the interaction between two neighboring chains of particles in a 2D crystal is weak and short range.

ACKNOWLEDGMENTS

We gratefully acknowledge support from the Department of Science and Technology, Govt. of India (SR/NM/NS-134/2010) and DST-PURSE. K.P.Z acknowledges the UGC for a fellowship. The authors also acknowledge support from Slovenian Research Agency under Contracts No. J1-6723 (I.M.), No. P1-0099 (I.M. and S.Č.), and No. Z1-6725 (S.Č.).

[1] P. Poulin, H. Stark, T. C. Lubensky, and D. A. Weitz, Science **275**, 1770 (1997).

[2] I. Muševič, M. Škarabot, U. Tkalec, M. Ravnik, and S. Žumer, Science **313**, 954 (2006).

[3] H. Stark, Phys. Rep. **351**, 387 (2001).
[4] R. P. Trivedi, D. Engstrom, and I. I. Smalyukh, J. Opt. **13**, 044001 (2011).
[5] O. V. Kuksenok, R. W. Ruhwandl, S. V. Shiyanovskii, and E. M. Terentjev, Phys. Rev. E **54**, 5198 (1996).
[6] P. Poulin, V. Cabuil, and D. A. Weitz, Phys. Rev. Lett. **79**, 4862 (1997).
[7] T. C. Lubensky, D. Pettey, N. Currier, and H. Stark, Phys. Rev. E **57**, 610 (1998).
[8] V. G. Nazarenko, A. B. Nych, and B. I. Lev, Phys. Rev. Lett. **87**, 075504 (2001).
[9] Y. Gu and N. L. Abbott, Phys. Rev. Lett. **85**, 4719 (2000).
[10] J. C. Loudet, P. Poulin, and P. Barois, Europhys. Lett. **54**, 175 (2001).
[11] P. G. Petrov and E. M. Terentjev, Langmuir **17**, 2942 (2001).
[12] M. Yada, J. Yamamoto, and H. Yokoyama, Phys. Rev. Lett. **92**, 185501 (2004).
[13] A. B. Nych, U. M. Ognysta, V. M. Pergamenshchik, B. I. Lev, V. G. Nazarenko, I. Muševič, M. Škarabot, and O. D. Lavrentovich, Phys. Rev. Lett. **98**, 057801 (2007).
[14] I. I. Smalyukh, O. D. Lavrentovich, A. N. Kuzmin, A. V. Kachynski, and P. N. Prasad, Phys. Rev. Lett. **95**, 157801 (2005).
[15] R. W. Ruhwandl and E. M. Terentjev, Phys. Rev. E **55**, 2958 (1997).
[16] M. Škarabot, M. Ravnik, S. Žumer, U. Tkalec, I. Poberaj, D. Babič, N. Osterman, and I. Muševič, Phys. Rev. E **77**, 031705 (2008).
[17] B. I. Lev and P. M. Tomchuk, Phys. Rev. E **59**, 591 (1999).
[18] O. Guzman, E. B. Kim, S. Grollau, N. L. Abbott, and J. J. de Pablo, Phys. Rev. Lett. **91**, 235507 (2003).
[19] M. Ravnik, M. Škarabot, S. Žumer, U. Tkalec, I. Poberaj, D. Babič, N. Osterman, and I. Muševič, Phys. Rev. Lett. **99**, 247801 (2007).
[20] I. Muševič, M. Škarabot, D. Babič, N. Osterman, I. Poberaj, V. Nazarenko, and A. Nych, Phys. Rev. Lett. **93**, 187801 (2004).
[21] M. Vilfan, N. Osterman, M. Čopič, M. Ravnik, S. Žumer, J. Kotar, D. Babič, and I. Poberaj, Phys. Rev. Lett. **101**, 237801 (2008).
[22] K. P. Zuhail, P. Sathyanarayana, D. Seč, S. Čopar, M. Škarabot, I. Muševič, and S. Dhara, Phys. Rev. E **91**, 030501(R) (2015).
[23] K. P. Zuhail and S. Dhara, Appl. Phys. Lett. **106**, 211901 (2015).
[24] M. Ravnik and S. Žumer, Liq. Cryst. **36**, 1201 (2009).
[25] C. Blanc, D. Svenšek, S. Žumer, and M. Nobili, Phys. Rev. Lett. **95**, 097802 (2005).
[26] See Supplemental Material at http://link.aps.org/supplemental/10.1103/PhysRevE.92.052501 to access video clips of the phase transition.